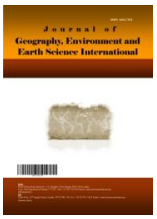

Journal of Geography, Environment and Earth Science International

24(2): 39-60, 2020; Article no.JGEESI.55452
ISSN: 2454-7352

Mapping of Pyroclastic Density Currents Hazards and Assessment of Related Risks by AMS Technique in the West-Cameroon Highlands: Case of Bambouto and Bamenda Volcanoes

Merlin Gountié Dedzo[1*], Ghislain Zangmo Tefogoum[2], Boris Chako Tchamabé[3], Eric Martial Fozing[4], Emmanuel Njonfang[5] and Pierre Kamgang[6]

[1]Department of Life and Earth Sciences, Higher Teachers' Training College, University of Maroua, P.O.Box 55, Maroua, Cameroon.
[2]Department of Earth Sciences, University of Maroua, P.O.Box 46, Maroua, Cameroon.
[3]CONACYT-Centro de Ingeniería y Desarrollo Industrial, Av. Playa Pie de la Cuesta 702, Desarrollo San Pablo, 76125, Querétaro, Qro., Mexico.
[4]Laboratory of Environmental Geology, University of Dschang, P.O.Box 67, Dschang, Cameroon.
[5]Laboratory of Geology, Higher Teachers' Training College, University of Yaoundé I, P.O.Box 47, Yaoundé I, Cameroon.
[6]Department of Earth Sciences, University of Yaoundé I, P.O.Box 812, Yaoundé, Cameroon.

Authors' contributions

This work was carried out in collaboration among all authors. Authors MGD and GZT designed the study, performed the statistical analysis, wrote the protocol and wrote the first draft of the manuscript. Authors BCT, EMF, EN and PK managed the analyses of the study and the literature searches. All authors read and approved the final manuscript.

Article Information

DOI: 10.9734/JGEESI/2020/v24i230202
Editor(s):
(1) Dr. Pere Serra Ruiz, Universitat Autònoma de Barcelona, Spain.
Reviewers:
(1) R. D. Elmore, University of Oklahoma, USA.
(2) Ali Amasha, Arab Academy for Science, Technology and Maritime Transport, Egypt.
Complete Peer review History: http://www.sdiarticle4.com/review-history/55452

Original Research Article

Received 19 January 2020
Accepted 24 March 2020
Published 07 April 2020

ABSTRACT

Ignimbritic flow deposits which derived from pyroclastic density currents (PDCs) are mostly observed in West-Cameroon Highlands located in the central portion of the Cameroon Volcanic Line (CVL), especially in Bambouto (21.12 - 0.50 Ma) and Bamenda (27.40 - 0 Ma) volcanoes.

**Corresponding author: E-mail: merlin.gountie@gmail.com, merlinodedzo@yahoo.fr;*

These deposits covering approximately 27% (≈195 km^2) of the volcanoes surface with thickness ranging from 30 to 200 m representing a total volume estimated at 20 km^3. Because of the intense weathering of the ignimbritic formations after their setting up and being buried by basaltic and trachytic flows, the initial volume of these pyroclastic deposits is really much larger. Soil fertility has fostered an important population growth (more than 1,200,000 people) in these volcanoes. The economic and agropastoral activities on the flanks and inside the caldera of the volcanoes are estimated at about $US7.5 billion. In this paper, we evaluate and realize cartography of the hazards associated to ignimbritic eruptions which are most disastrous in term of volcanic process in this region. Magnetic studies, specifically, Anisotropy of Magnetic Susceptibility (AMS) method has been utilized for the determination of flow directions in visually nearly isotropic ignimbritic deposits outcrops. The AMS data reported from the Bamenda and Bambouto volcanoes ignimbrites produced significant informations about the depositional scheme of the PDCs. In most sites, magnetic lineations and principally magnetic foliation are reliably parallel to downhill directions, frequently with an upslope imbrication. Inferred palaeoflow directions based on the field indicators, orientation of minerals and other objects in oriented thin sections and the directional AMS data show that Bambouto caldera, Oku crater and Santa-Mbu caldera are the sources of main PDCs of Bambouto and Bamenda volcanoes. These AMS results have aided us to produce a hazard and risks maps related to potential future pyroclastic flows on these volcanoes. The assessment of risks in these volcanoes was based on populations in the study area, infrastructures (houses and roads) and average income of breeding activity.

Keywords: Bambouto and Bamenda volcanoes; ignimbrites; anisotropy of magnetic susceptibility; hazard and risk maps; assessment.

1. INTRODUCTION AND BACKGROUND GEOLOGY

The Cameroon Volcanic Line (CVL) is an alignment of continental and oceanic volcanic massifs, and plutonic complexes spreading from Pagalu island in the Atlantic Ocean to lake Chad (Fig. 1). The volcanism along the CVL is still active at Mount Cameroon with the 1999 and 2000 eruptions. Volcanic activities in this line started during the Eocene with the setting up of the Bamoun plateau between 51.8 and 46.7 Ma [1] and Mount Bangou between 44.7 and 43.1 Ma [2]. Rhyolites, phonolite, trachyte and basalt are the main products of this volcanism [3,4,5,6,7,8,9,10,11]. Ignimbrite outcrops are found only in the central continental part of the CVL, particularly in the Bamenda and Bambouto volcanoes [12,13,14]. In Nkogam massif, other small deposits are also reported [14,15,16, 17,18,19].

Mount Mélétan (2740 m) and Bambili Lake borders (2621 m) are the highest point of the massif (Fig. 2) of the Bambouto and Bamenda volcanoes respectively which cover an area of about 1400 km^2. The presence of PDCs deposits (Fig. 3) justify the hazard caused by the volcanoes which are still considered as an active with a 0 Ma basalts in Mt Bamenda [20] and 0.480 Ma scoriae in Mt Bambouto [21].

Bamenda volcano is made up of two calderas namely, Santa-Mbu caldera (6 x 4 km) and Lefo caldera (4 x 3 km). Their floors and external slopes are composed principally by domes and lava flows of trachytic nature. According to Kamgang et al. [7,20,22], felsic and intermediate rocks (27.40 - 18.98 Ma) are made of rhyolites, trachytes, benmoreites and mugearites. Mafic rokcs (17.4 Ma to the present) are represented by hawaiites, basalts and basanites. Welded and non-welded ignimbrite deposits are generally lie on the granito-gneissic basement and covered by lateritized old basalts.

The volcanic products of Bambouto volcano (21.12 to 0.48 Ma) consists of rhyolite, phonolites, trachytes, basalts and various facies of ignimbritic deposits [4,16,21,23,24, 25,26,27,28]. The Mt Bambouto caldera is situated in the summit of the volcano and represents an irregular depression with an elliptical form (16 x 8 km). Subvertical walls on the southeast side and the dregs of this caldera are characterized by trachytic and phonolitic flow-domes and domes.

1.1 Pyroclastic Density Currents Deposits

PDCs constitute an inhomogeneous combination of lava fragments, ash, block and gas that flow according to their density relative to the nearby

fluid and due to Earth's gravity [29,30]. The deposits of these PDCs lead to the formation of ignimbrite. Temperatures (up to 600-700°C) and speeds (up to 300 km/h) of these flows are generally high on the earth surface [31,32,33,34,35], and frequently implying a turbulent regime [32,36,37,38]. When a PDCs have a solid volume concentration equal or less than a few percent, it's a diluted pyroclastic flow; a concentrated suspension or of high concentration will therefore have a concentration of several percent or several tens of percent [39]. Diluted concentration flows with stratified deposits which drape topography are known as pyroclastic surges. Pyroclastic flows are generally denser than pyroclastic surges and form more massive poorly sorted deposits that fill valleys and poorly sorted [40,41,42,43]. Pyroclastic surges can be associated with a pyroclastic flow, situated at the edge of this flow or produced by ash cloud surmounting it (case of Mt. St. Helens [44] and the Soufriere Hills

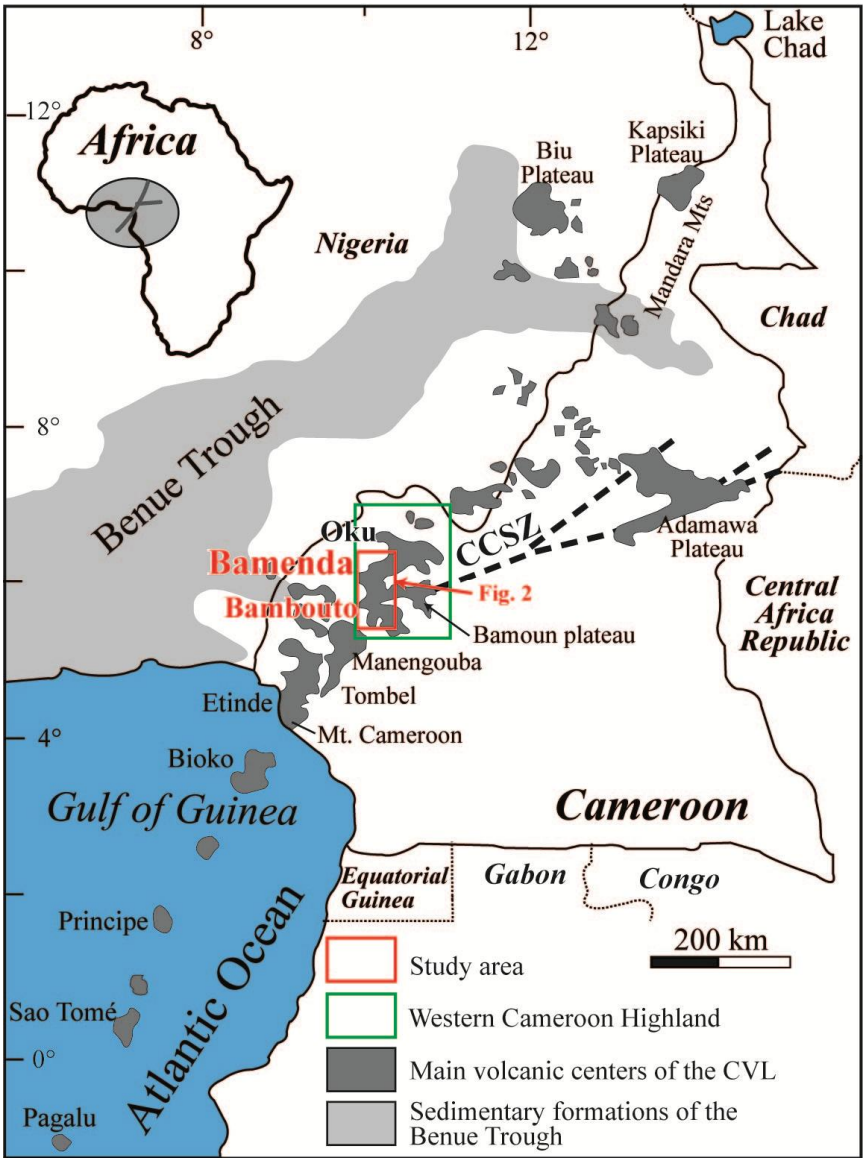

Fig. 1. Location of the study site in the Cameroon Volcanic Line (CVL); Inset: location of the CVL in Africa

OVG: Oku Volcanic Group; WCH: Western Cameroon Highland; CCSZ: Central Cameroon Shear Zone according to Ngako et al. [19]

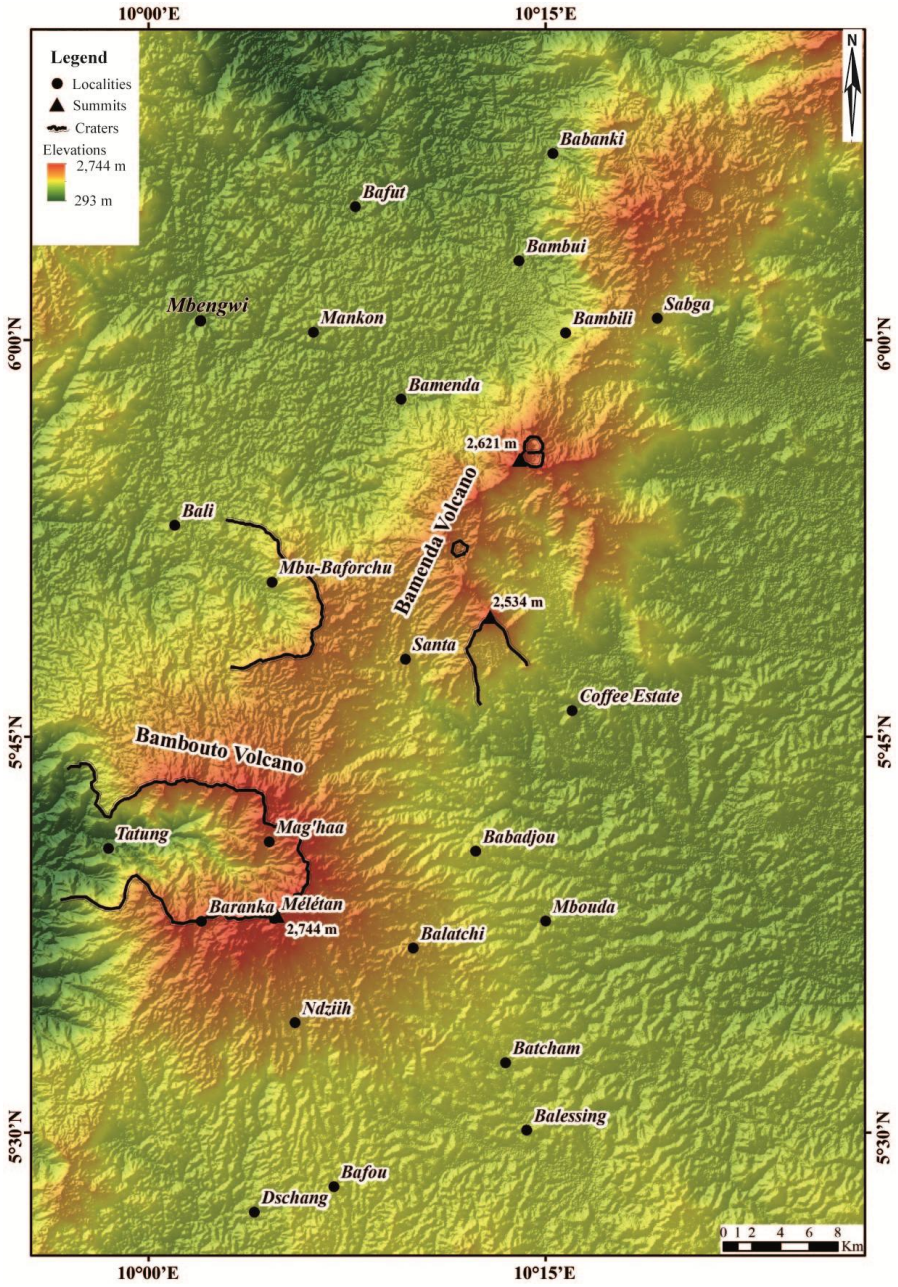

Fig. 2. Digital elevation model (DEM) of Bambouto and Bamenda volvanoes: Shuttle Radar Topography Mission (SRTM, NASA)

volcano [45]). These two categories of flows deposits have been identified on Mts Bamenda and Bambouto. They can originate from laterally inclined blasts or from hot avalanches resulting from lava domes, or by fountain-like downfall of parts of an eruption column following explosive fragmentation of rock and magma in a volcanic conduit. PDCs can transport important volumes of hot debris speedily for several kilometers across the ground and they represent a destructive and lethal volcanic hazard. Ground-hugging PDCs create a buoyant counterpart, known as co-ignimbrite ash plume or a phoenix cloud, which can transport aerosols and ash into the stratosphere and thus can cause important climatic malfunction. The majority of processes within PDCs is difficult to observe and are frequently inferred from the related deposits.

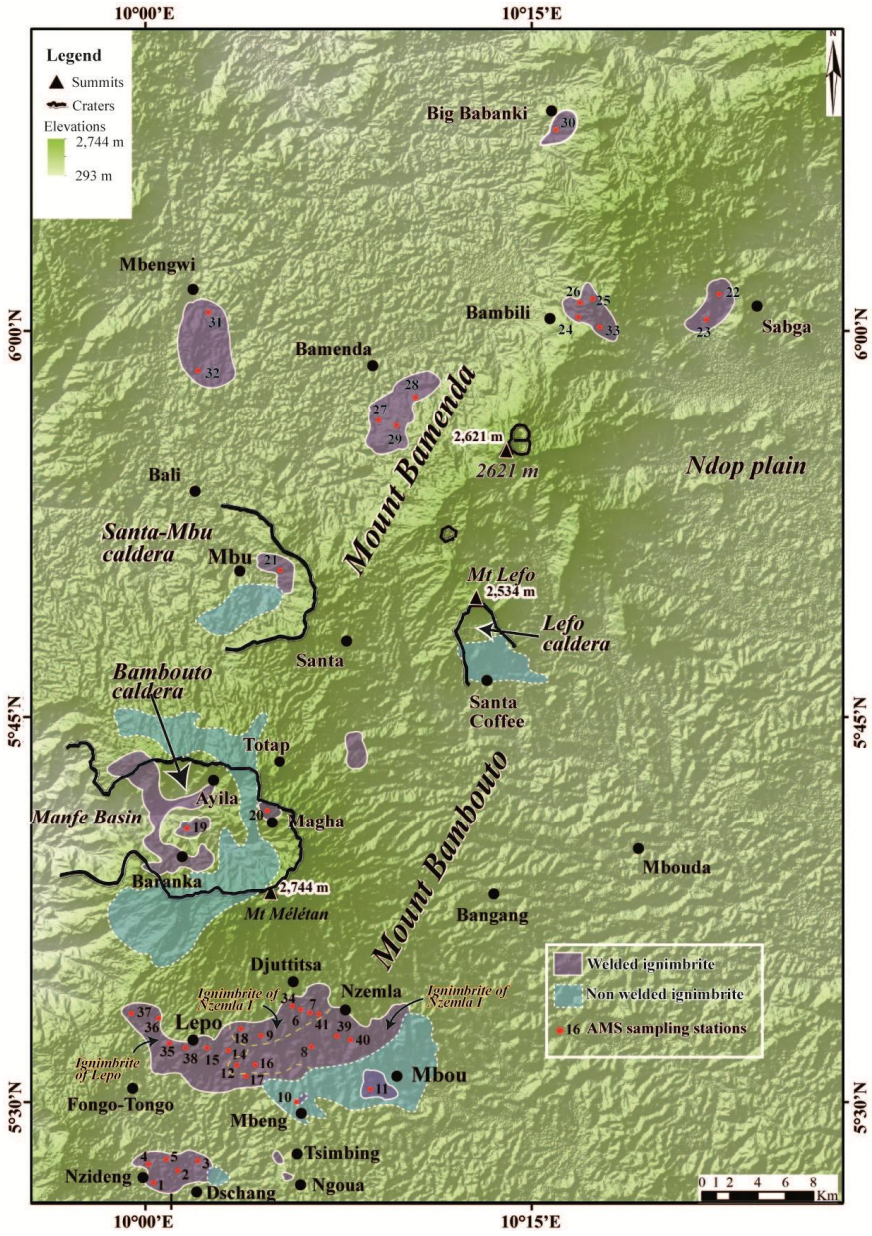

Fig. 3. DEM of study area presenting the ignimbritic outcrops (modified from Gountié dedzo et al. [13]) and the AMS sampling stations

1.2 Aim of Study

A significant number of people have been killed on volcanoes during the previous few decades by somewhat small volcanic eruptions that otherwise represented no hazard to nearby cultivated and populated areas. PDCs have caused about 65,000 deceases since 1600 A.D. (about 48% of all volcano-related fatalities). The Bamenda and Bambouto volcanoes are considered as active and can possibly cause enormous damage if an eruption happened, since in the past, violent eruptions have resulted in substantial ignimbrite deposits in the calderas and on the slopes of the volcanoes. The aims of this manuscript are to cartography and assess PDCs hazards at Mounts Bamenda and Bambouto which are the most catastrophic in terms of possible volcanic processes. To accomplish this objective, AMS has been used to infer palaeoflow directions in ancient deposits of ignimbrite which, are visually practically isotropic

in all outcrops. Results of magnetic fabrics of ignimbritic deposits aid us to determine ancient flow directions of PDCs, to reassemble discontinuous deposits into their primary ignimbrite sheets, and to locate their emission source. Such restorations permit us to predict scenarios of future probable ignimbritic eruption and to realize a vulnerability, hazard and risks maps of PDCs in the Bamenda and Bambouto volcanoes.

2. FIELD OBSERVATIONS AND PETROGRAPHY OF IGNIMBRITES

Ignimbrites are principally observed in the central portion of the CVL; they are located predominantly in Mt Bambouto and its NW extension (Mt Bamenda) (Fig. 2). The Bambouto ignimbrite deposits (about 17% of the massif) (Fig. 2) outcrop sporadically and represent roughly 135 km^2 for a total volume projected at 13.65 km^3. The ignimbrites of Mt Bamenda represent approximately 7.5% of the rocky outcrops of the volcano constituting about 45 km^2 with a volume of around 6.42 km^3 (Fig. 3). These volumes are actually much higher because these formations are generally covered by lateritized basalts. In the two volcanoes, ignimbrites are covered by lateritized basalt and lie on a basement made up of granitoid and gneiss. The different facies are principally massive lithic breccia facies (mlBr) and massive lapilli tuff (mlT) according to Kokelaar and Branney [29] classification.

These ignimbritic deposits are characterized by their high aspect ratio of about 3.2 x 10^{-2} to 1.5 x 10^{-2} in Mt Bambouto and 7.23 x 10^{-2} to 2.77 x 10^{-2} in Mt Bamenda. In fact, the shape of an ignimbrite sheet may, apart from its volume, be basically and quantitatively described by the aspect ratio which is defined as the ratio of average sheet thickness to the diameter of a circle that covers the similar area as the sheet [40,46,47]. The aspect ratios of the studied ignimbrites range from > 10^{-2} (high aspect ratio) to < 10^{-5} (low ratio). We distinguish in the field the welded and non-welded ignimbrites depending to the degree of welding.

2.1 The Welded Ignimbrites

The welded ignimbritic deposits generally outcrop as sheets. Depending of the type of the facies, the colors of rock are whitish, dark gray and light gray with massive and compact structure. In the ignimbrites of Bamenda volcano, the amounts of minerals and lithic fragments are considerably less significant compare with those of neighboring Mt Bambouto [12].

Ignimbrite deposits in the two volcanoes are generally made of two or one flow units which consist of a simple cooling unit [12]. The fiammes (5-20%) which is lens or flame-shaped object, such as typically forms from flattened lapilli-rich pumice in a welded ignimbrite, presents lenticular to ovoid shapes. Eutaxitique fiammes with unidirectional orientation are present at Nzemla and Bambili localities. Trachytic enclaves (10-20%) are the main component of the lithic fragments of mlT ignimbrites. In Mbou, Big Babanki, Mbu and Mbengwi municipalities were the mlBr facies are represented, enclaves of black scoriae (20-25%) constitute the majority of the rock fragments. Enclaves of granite, scoriae, ignimbrites and vitrophyres are less represented (1-5%). Devitrified matrixes (50-90%) are made up of clinopyroxene (1%), plagioclase (1%), oxides (1-2%), biotite (2%), quartz (2-5%) and alkali feldspar (10-35%; sanidine and anorthoclase).

2.2 The Non-welded Ignimbrites

The non-welded ignimbritic deposits are volcanic tuffs and also belong to Tlm facies. These deposits cover about 65 km^2 of the massifs (Fig. 2) [12]. The rocks outcrop in Dschang, Mbeng Santa Coffee and in the calderas of the two volcanoes (Bambouto caldera, Santa-Mbu and Lefo caldera). Due to the abundant vegetation and uneven terrain the exact thickness (> 20 m) of non-welded ignimbrites is difficult to assess. This facies is very powdery and mainly consists of trachytic enclaves (20-25%) with insignificant proportion of rhyolite, ignimbrite, obsidian and granite. The mean size of these lithics is 3 x 2.4 cm. The dimension of some trachytic lithic fragments reached 4.5 x 6 m in Bambouto caldera and 1.5 x 2.5 m in Lefo caldera; these huge lithic rock fragments are comparable to co-ignimbritic breccias and generally linked with subsidence related to the genesis of calderas. Agglomerated volcanic ash (accretionary lapilli; up to 10%) with variable size (0.6 to 2.5 cm in diameter) are also present in all non-welded Tlm facies. The matrix of non-welded ignimbrites constituted by ashy fine particles represents 25-30% of these formations.

3. SAMPLING METHOD AND AMS MEASUREMENTS

The magnetic susceptibility (K) of a rock refers to its response to an applied magnetic field.

Magnetic susceptibility (K = M/H, in SI: international system of units) also expresses the ability of a body to acquire a magnetization (M) when subjected to an inducing magnetic field (H). K is a scalar for an isotropic body ($K_1 = K_2 = K_3$), but if this body is anisotropic ($K_1 \geq K_2 \geq K_3$) then there is anisotropy of magnetic susceptibility. Iron is the principal element responsible for the magnetic susceptibility. AMS predominantly defines grain-shape anisotropy for magnetite. AMS also expresses crystallographic control on magnetic properties for other minerals. Therefore, we may infer the orientation-distribution of a main mineral from the AMS of a rock. Flow-directions from PDCs deposits and magma, current directions from sediment, can be recorded by AMS principal directions [12,35]. In this paper, AMS is applied to PDCs deposits or ignimbrites with an aim to reconstruct palaeoflow directions of pyroclastic current. All AMS data were acquired at Paul Sabatier University in Toulouse (France) in GET (Géosciences Environnement Toulouse) laboratory. Sampling of the the Bambouto volcano (244 core samples) and Bamenda volcano (115 core samples) ignimbrites was done on 41 sites (Fig. 3) using a non-magnetic diamond-tipped drill bit portable, gasoline-powered drill-machine. Samples were only taken from nearly horizontal beds (dip less than 10°) and from rocks with a grain size smaller than that of ash (< 2 mm). At each station, a total of 6 to 10 oriented cores were collected in a surface covering about 4 to 8 m^2. None of the studied rocks showed field evidence of rheomorphic flow (secondary flow) that might have modified their primary emplacement magnetic fabric. Before numbered samples, Magnetic compass was used to orientate (azimuth/dip). Each core sample in laboratory was severed into 22 x 25 mm cylindrical specimens, using a non-magnetic, diamond tipped saw blade. A total of 297 specimens were obtained with up to four specimens per sample. AMS measurements were done on a KLY-3S Kappabridge susceptometer (Agico, Czech Republic) working at low alternating field (4×10^{-4} T at 920 Hz) with a sensitivity of about 2×10^{-7} SI, tolerating anisotropy discrimination below 0.2% over a large range of susceptibility. This technique measures the orientation of the minerals (magnetic carriers) in a rock sample which aid to restore palaeoflow directions. In different directions of the sample, the AMS can also be measured and the results are generally expressed in terms of a triaxial ellipsoid characterized by the minimum, intermediate and maximum susceptibility directions, Kmin Kint and Kmax respectively. The anisotropy of the principal susceptibility axes is commonly considered to be inherited from the mechanism of emplacement and can be used to reconstruct flow directions in intrusions, lavas and ignimbrites. The minimum susceptibility (short axis K_3) represents the pole of foliation, meanwhile the maximum susceptibility (long axis K_1) characterize the magnetic lineation; the mean susceptibility is define by K_2 axis. Km (average of magnetic susceptibility) expresses the arithmetic mean of the main axes (Km = [K1 + K2 + K3] / 3). The (Km) is of the lengths. The method also estimates P% (anisotropy percentage; P% = [(K1 / K3) − 1] × 100), F% (planar anisotropy (F% = [(K2 / K3) − 1] × 100) and L% (linear anisotropy; L% = [(K1 / K2) −1] × 100). The T parameter express by $T = (2\ln K_2 - \ln K_1 - \ln K_3) / (\ln K_1 - \ln K_3)$ characterize the shape of the susceptibility ellipsoid [48] and fluctuating from -1 for prolate ellipsoid to +1 for oblate ellipsoid. The values of T ranging between +0.5 and -0.5 qualify the triaxial ellipsoids.

Numerous researches have used AMS in an attempt to localize source vents of large ignimbritic deposits since the early study of Elwood [49]. Several researchers [50,51,52] compared AMS data from PDCs deposits with petrographic and field observations and recognized that AMS provides a significantly rapid and precise means of assessing the transport direction of ignimbrites than macroscopic examination techniques. It is confirmed that the heterogeneous character of an ignimbritic deposits does not completely affect the fabric of AMS, and that AMS offers a realistic indication of the PDCs flow direction [53,54]. The shape of the AMS ellipsoid of most rocks characterizes the favorite alignment of paramagnetic (Km < 500 µSI) and ferromagnetic (Km > 500 µSI) mineral grains within the rock [49,55]. Numerous AMS studies have revealed that ferrimagnetic phases such as maghemite and magnetite, dominate the magnetic susceptibility when these phases are present in silicic rocks [56,57,58]. The mean plane of magnetic foliation (represented by K_1–K_2 axes) is normal to the K_3 axis and approaches the flow plane in the case of a normal magnetic fabric. Nevertheless, the plane of magnetic foliation frequently differs in orientation (imbrication angle) comparative to the flow plane [49,50,59] and inclines in a direction opposite to the direction of flow. The imbrication dip direction is supposed to point towards the emission center or source area of PDCs (Fig. 4). The K_1 axis is

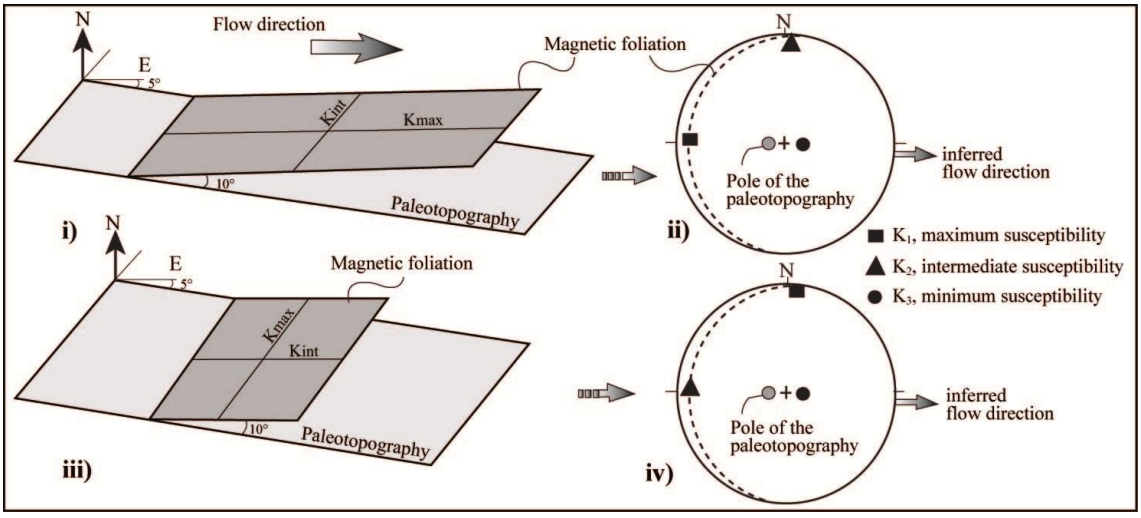

Fig. 4. Conceptual model for imbrication of magnetic foliation in two ideal cases; (i) Magnetic foliation can be imbricated with Kmax axis oriented parallel and (ii) perpendicular to the flow direction, and the related (iii, iv) stereoplots of AMS axes. Note the orientation of the magnetic foliation is parallel to the inferred flow direction in both cases (redraw from Giordano et al. [59])

usually inferred to be parallel to the direction of flow and therefore plunges towards the emission center [50]. A different methodology must be used to interpret the AMS data because the use of the maximum susceptibility axis K_1 alone as a proxy for flow direction is not usually reliable [50,52,60,61,62]. Another method to determine the flow direction of PDCs deposits is the use of the imbrication angle of the plane of the magnetic foliation, which equals the deviation of the minimum axes K_3 from the normal to the macroscopic flow plane [63,64,65] (Fig. 4). In the present study, the K_1 axes are roughly perpendicular to the dip direction of the imbrication plane in most AMS sites then, only the K_3 axes were used to infer flow directions in the case of normal fabrics. According to Wang et al. [66], the AMS fabrics is (i) normal when the magnetic foliation is subhorizontal (K_1 axis dips at angle of less than 30°) and (ii) inverse when the magnetic foliation plane is subvertical (K_1 dips at high angle generally > 50°). Inverse fabrics have been attributed to secondary processes [67], such as hydrothermalism or post emplacement modification (tectonic effect). Concerning the ignimbrites of Bambouto and Bamenda volcanoes, post-depositional vertical structures are attributed to subvertical elutriation pipes [12]. In fact minuscule secondary oxide minerals may have deposited or be crystallized in the pore boundaries produced from separation and upwards movement of dust-loaded vapor phases formed during post-emplacement of ignimbrites [12].

4. RESULTS OF AMS AND DISCUSSION

4.1 Identification of Emission Centres

In the two volcanoes, inverse AMS fabrics were not used to infer flow direction of PDCs; but in some cases (GM7, GM29 and GM40) presenting this type of fabric, orientation of minerals and other objects (fiammes, rock enclaves and minerals) in oriented thin sections (Fig. 5) were used to determine transport direction following the procedure of Robin [68] and Launeau and Robin [69].

4.1.1 Bambouto volcano

All AMS stations of Lepo display normal fabrics (Table 1, Fig. 6) with best pole of synthetic stereograms of magnetic foliation and a best line of magnetic lineation at 190/84 and 43/3 respectively. Three stations have planes of magnetic foliation gently inclined (2-10° for GM36, GM37 and GM38) to NE, whereas station GM35 show K_3 axe inclined approximately 10° to E. The remaining stations are imbricated to the NW (3 to 28°), as can be observed in Fig. 6. Magnetic lineations commonly present a NE-SW direction with low plunges (2 - 6°). AMS directions and field transport evidently indicate

that the source of these PDCs is located in the Mt Bambouto Caldera (Figs. 6 and 8).

Stations of Dschang ignimbritic deposits also present normal fabrics (Table 1, Fig. 6). Magnetic lineations (low plunges: 1 - 10°) define a NE-SW axis with the best line and the best pole of magnetic foliations at 38/4 and 248/88 respectively. The general flow direction for Dschang PDCs deposits (stations GM3, GM2, GM1), inferred by field indicators (imbricated fiammes nearby station GM1 with N56°E mean direction) and magnetic data suggest that flow was moved to SW (Figs. 6 and 8). The AMS data

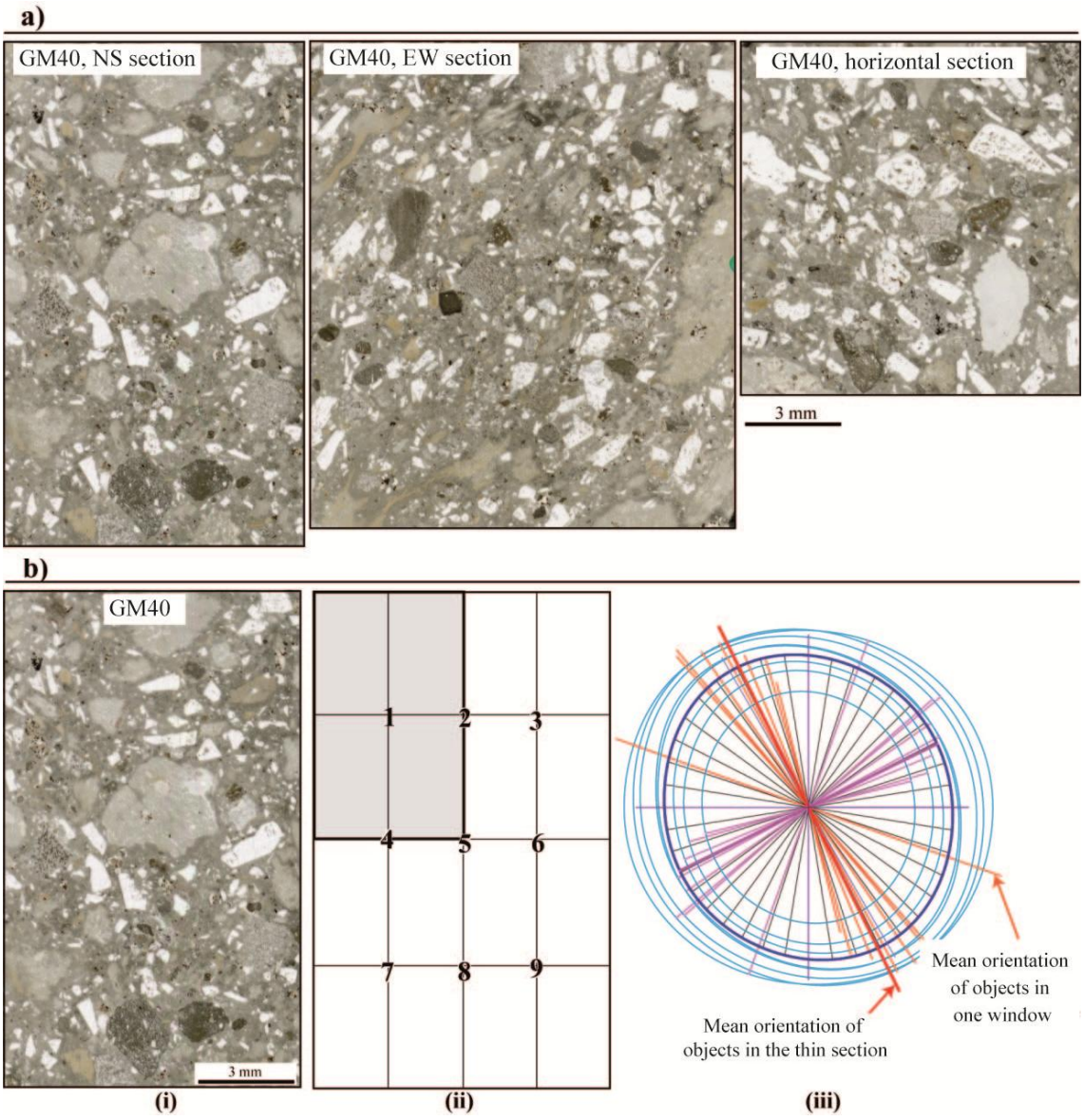

Fig. 5. Determination of the shape fabric ellipses. a) Oriented thin sections realized from sample GM40 following the NS, EW and horizontal sections. b) Exemple of the acquisition of the shape fabric ellipses using the intercepts method following the procedure of Robin [68] and Launeau and Robin [69] from (i) one thin section realized in NS plane; (ii) with nine overlapping windows of the thin section, (iii) mean ellipse (dark blue circle) of the shape fabric is obtained from the nine ellipses (light blue circles) of all windows. In the thin section, objects are represented by fiammes, rock enclaves and minerals

Table 1. Magnetic study results of Bambouto and Bamenda volcanoes. N is the number of samples for the site; Km is the mean magnetic susceptibility; L% is the linear anisotropy percentage; F% is the planar anisotropy percentage; P% is the total anisotropy percentage; T is the Jelinek's shape parameter [48]; K_1, K_2 and K_3 are the maximum, intermediate and minimum susceptibility intensities respectively; D: declination in degrees; I: inclination in degrees

Locality	Site	N	AMS parameters					Means eingenvectors					
								K_1		K_2		K_3	
			Km (μSI)	P%	L%	F%	T	D	I	D	I	D	I
Bambouto volcano													
Dschang	GM02	24	1763.5	7.1	1	6	0.7	31	7	121	0	212	83
	GM04	27	1712.9	8.2	0.8	7.3	0.8	224	1	134	6	325	84
	GM05	18	2198.8	6.3	0.3	6	0.9	208	2	298	6	102	83
	GM01	23	196.6	2.5	0.1	2.3	0.9	70	10	161	2	264	80
	GM03	23	195.7	0.3	0	0.3	0.8	18	10	287	1	190	80
Mbou	GM11b	9	250.5	1.9	0.3	1.7	0.7	359	23	260	18	154	68
Mbeng	GM10	22	187.8	0.5	0.2	0.3	0.3	132	65	330	24	237	7
Lepo	GM13	22	571.7	3.7	0.4	3.2	0.8	71	2	341	12	168	78
	GM14	23	512.9	0.2	0.1	0.1	-0.3	41	3	310	18	139	72
	GM15	17	1303.4	0.3	0.1	0.2	0.6	26	4	295	8	143	81
	GM17	23	419.1	2.1	0.3	1.8	0.7	43	2	313	3	163	87
	GM38	32	801.5	1.9	0.1	1.7	0.8	60	5	330	8	182	80
	GM35	27	211.2	1.1	0.1	1	0.9	27	6	118	8	261	80
	GM36	33	614.4	3.5	0.2	3.3	0.9	77	4	347	2	233	86
	GM37	27	130.6	0.4	0.1	0.3	0.6	334	2	64	2	208	88
Nzemla I	GM06a	10	819.1	0.4	0	0.4	0.8	324	56	195	23	94	24
	GM06b	10	856.9	0.4	0.1	0.3	0.5	285	51	25	8	121	38
	GM06c	8	952.5	0.4	0.1	0.4	0.7	302	45	168	35	59	24
	GM07	9	359.1	1	0.4	0.6	0.1	59	4	328	8	179	81
	GM09	17	1610.5	0.2	0	0.1	0.6	35	75	265	10	174	11
	GM18	21	3473.2	0.2	0	0.2	0.9	127	4	216	1	283	86
	GM34	35	3374.7	0.2	0.1	0.1	0.1	19	10	286	17	139	70
	GM41	16	227.3	0.2	0.1	0.1	0.0	107	81	304	8	214	3
Nzemla II	GM08	25	153.7	0.3	0.2	0.1	-0.2	215	75	84	10	352	12
	GM12	20	24.2	1.2	1	0.3	-1.0	309	75	54	4	145	15
	GM16	24	211.1	0.7	0.5	0.2	-0.6	238	80	132	3	42	10
	GM39	24	107.5	0.7	0.7	0.1	-0.7	230	86	4	3	94	3
	GM40	20	99.8	0.5	0.3	0.2	-0.6	177	74	274	2	4	16
Baranka	GM19	17	354.7	2	0.4	1.6	0.7	335	26	72	15	188	60
	GM20	25	703.7	1.1	0.7	0.4	-0.3	7	47	221	37	117	18
Bamenda volcano													
Bamenda	GM27	23	147.3	0.7	0.3	0.4	0.1	142	2	233	11	45	79
	GM28	24	88.9	0.7	0	0.7	0.9	254	35	14	35	134	36
	GM29	22	375.5	0.6	0.4	0.2	-0.3	278	81	43	6	134	8
Mbu	GM21	20	911.1	0.8	0.3	0.4	0.1	213	13	307	13	79	71
Mbengwi	GM31	33	2062.5	0.2	0	0.1	0.5	182	24	274	4	12	66
	GM32	32	725.6	1.4	0.1	1.2	0.8	197	1	100	13	310	87
Bambili	GM24	24	3253.2	0.2	0	0.2	0.6	315	2	45	6	202	84
	GM26	12	2579.5	0.2	0.1	0.1	0.0	50	26	144	8	249	62
	GM33	27	66.6	0.1	0.1	0.1	0.1	39	84	290	2	199	6
Sabga	GM22a	11	1220.6	1.7	0.7	1	0.2	315	32	73	37	197	37
	GM22b	9	1143	1.6	0.5	1.1	0.4	128	20	241	47	23	36
	GM23a	7	391.9	0.5	0.3	0.1	-0.3	221	8	340	73	129	15
	GM23b	9	379.8	0.5	0.2	0.3	0.0	225	6	116	73	317	16
Big-Babanki	GM30	12	55.5	0.5	0.2	0.3	0.0	56	6	326	0	235	84

Source: [73]

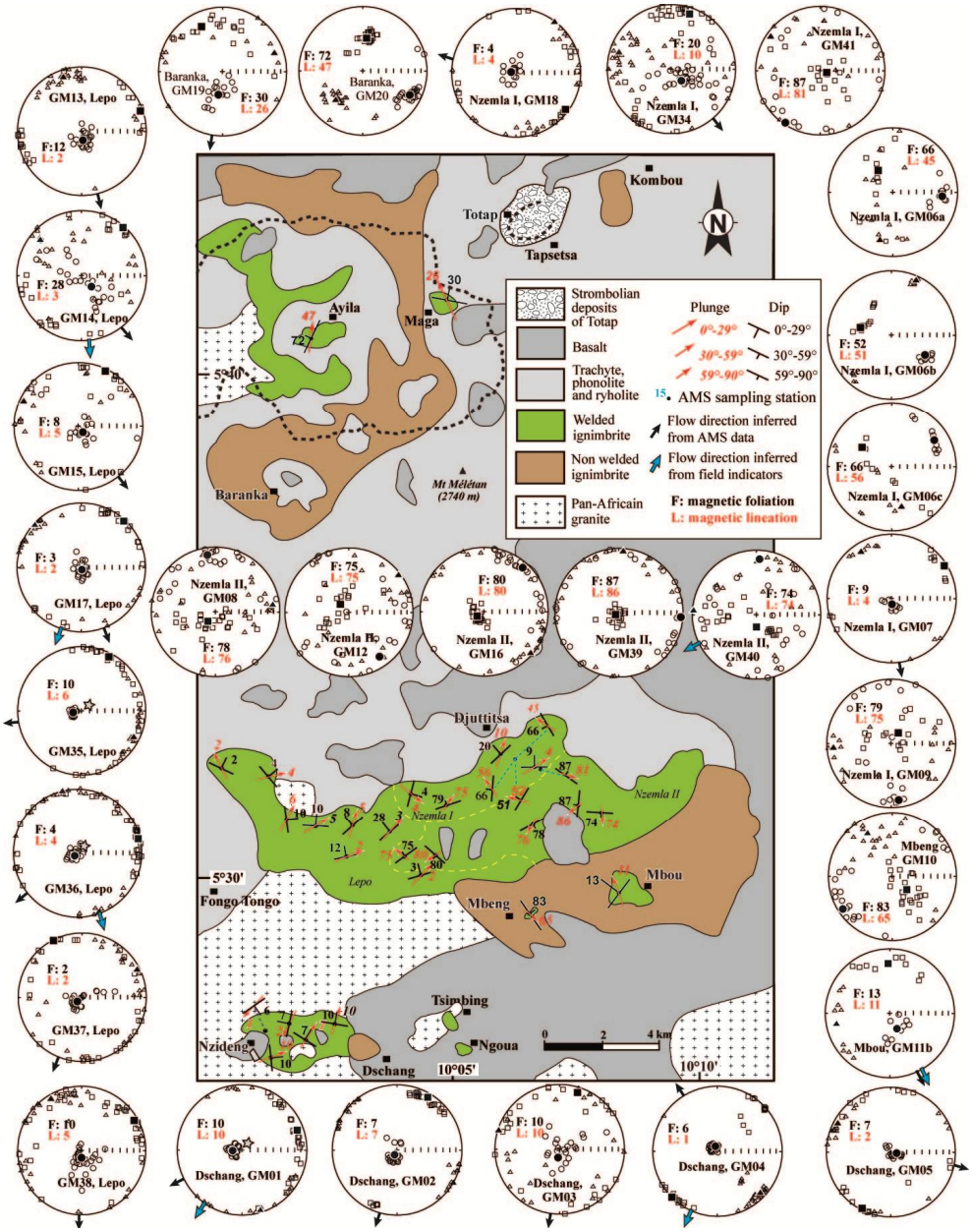

Fig. 6. Magnetic lineation and magnetic foliation map obtained from AMS stations of Bambouto volcano ignimbrites. Lower hemisphere projections of AMS data from Mt Bambouto with inferred flow direction using field indicators and imbrication of magnetic foliation (normal fabrics) are also shown; squares, triangles and circles represent K_1, K_2 and K_3 respectively; filled symbols represent means of K_1, K_2 and K_3; stars represent the pole of the paleotopography. In every stereoplots of AMS axes, values of magnetic foliation (F) and lineation (L) are also given

for the remaining two sites (GM5 and GM4) are practically orthogonal to the general flow direction. Modification of K_1 directions and in the flow imbrications angle in the study area thus expresses variations in local slope which increases the global scattering of the transport directional data. The influence of subtle topography on directional data of AMS has been in fact recognized in other PDCs deposits [70,71,72].

Eight AMS sites at Nzemla I show K_3 and K_1 axes slightly dispersed with an overall trending to the SE and NW (best pole of magnetic lineation and foliation are 23/9 and 154/77 respectively. In detail, three sites (GM7, GM18 and GM34) show normal fabrics with a poorly defined flow direction toward the SE to the W, consistent with field data suggesting transport toward the SW at station GM7. The other 5 stations display inverse fabrics with abruptly dipping planes of foliation (52-87°) and reasonably to extremely plunging lineations (45-81°). General flow direction inferred from normal AMS fabrics is to SE (Figs. 6 and 8), consistent with flow direction infer from imbricated lithic fragments around station GM11 (with N49°E mean direction) and from orientation of minerals and other objects in oriented thin sections (Fig. 5) also evidently indicate Bambouto caldera as the emission center of these PDCs deposits (Figs. 6 and 8).

Due to the inverse magnetic fabrics at Baranka, Mbeng and Nzemla II (Table 1, Fig. 6), no transport direction can be identified. The five stations of Nzemla II display subvertical plane of foliation (75° - 87°) and high plunges of magnetic lineation (51° - 86°). In station GM40, orientation of different objects and minerals in oriented thin sections suggest a NW - SE flow direction (Fig. 5). GM10 station, at the Mbeng also displays high plunge of lineation (65°) and high magnetic foliation dip (83°). Site GM19 displays a reasonably dipping plane of magnetic foliation (30°) and a transverse-to-flow magnetic lineation (26°). At Baranka, site GM20 in Bambouto caldera shows moderate plunge of magnetic lineation (47° to the north) with a subvertical magnetic foliation (72°).

AMS station of Mbou with a normal fabric (GM11b) was used to have an idea of the transport direction. In fact, the pole of magnetic foliation points to the NW, signifying a NW - SE flow. Imbricated lithic fragments nearby this site are consistent with this flow direction (Figs. 6 and 8).

Based on magnetic foliation, imbrication of field indicators and orientation of minerals and other objects in oriented thin sections, we finally conclude that the PDCs responsible for these ignimbritic deposits were generated from caldera of Bambouto volcano.

4.1.2 Bamenda volcano

AMS directional data indicate a relatively consistent transport pattern in different stations inferred by magnetic foliation plane or imbrication dip direction. The most stations located at Big Babanki, Bambili, Mbengwi, Mbu and Bamenda show normal fabric (Table 1, Fig. 7) characterized by well-defined magnetic fabrics presenting generally moderately inclination (3 - 24°) of the planes of magnetic foliation and low plunges (1 - 26°) of the magnetic lineations. The remaining seven staions at Sabga, Bambili and Bamenda cannot used to suggest the transport direction of flow since they display inverse fabric characterized by commonly abruptly dipping magnetic foliation planes (52 - 82°) and extremely plunging (20 - 81°) of magnetic lineations.

AMS sites at Mbu, Mbengwi and Bamenda with well-defined normal fabric (excepted stations GM28 and GM29 with inverse fabrics), field indicators imbrication (GM28) and orientation of minerals and other objects in oriented thin sections (GM29) demonstrate that flow direction of PDCs is from SW to NE. Therefore, Santa-Mbu caldera is the probable source of the Bamenda, Mbenwi and Mbu ignimbrites (Fig. 8).

Concerning the AMS stations of Big Babanki, Sabga and Bambili, only 3 sites exhibits normal fabrics (Bambili: GM24, GM26; Big Babanki: GM30) and can be used to infer flow direction. The imbrication of fiammes and others lithics in Sabga (GM22) and Bambili (GM24) ignimbritic deposits was also used to suggest transport direction. It's obvious that flow patterns of PDCs were roughly directed from NE to SW; we can then conclude that PDCs responsible for the ignimbrite deposits of Babanki, Sabga and Bambili were probably generated from Oku caldera located in the NE of these localities (Fig. 8).

4.2 Mapping and Assessment of the Ignimbritic Hazards

4.2.1 Mapping

With outcrop map of exposed ignimbritic deposits and their thickness, we have drawn hazard map (Fig. 9) related to PDCs or ignimbrite eruptions which are responsible for these deposits. In the zones where ignimbritic deposits are covered by other volcanic rocks, the boundary and approximately thickness of PDCs deposits were evaluated from several roadcuts, quarries (for engineering materials or construction), wells and particularly from water drillings, realized on trachytic and basaltic covers. The drillings carried out in these zones are in noteworthy numbers

(over 290 listed in the study area) and deeper than 40 meters in many cases. The data collected (thickness of PDCs) have permitted to evaluate in more realistic manner, the surface, the volume of ignimbrites and reliable hazard map. According to the data acquired from the AMS technique and the field studies of pyroclastic deposits in the volcano's craters and on their respective slopes, the former flows have been mapped. It emerges that the steepest slopes of the volcanoes controlled the flow of the pyroclastic materials [73].

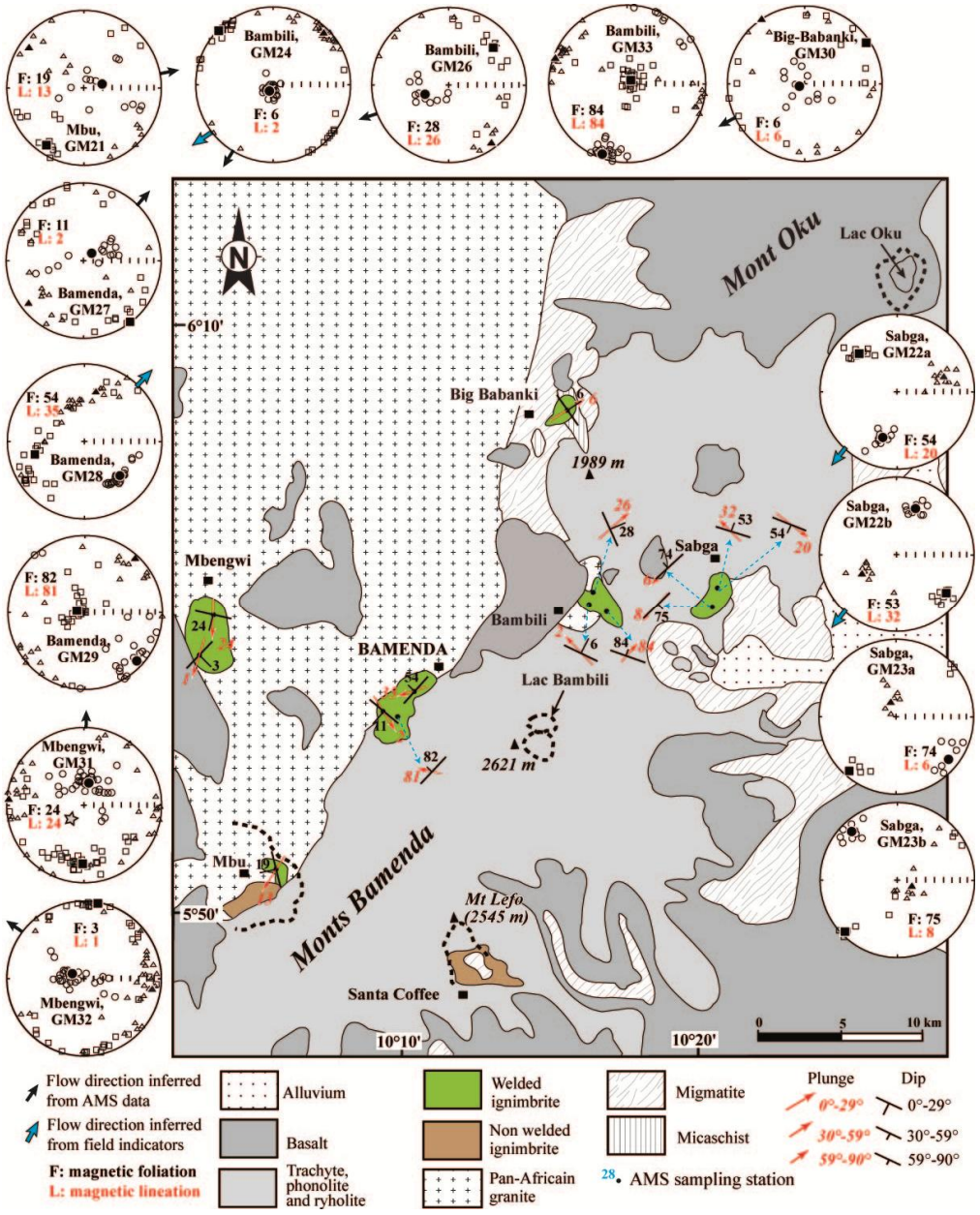

Fig. 7. Magnetic lineation and magnetic foliation map obtained from AMS stations of Bamenda volcano ignimbrites. Lower hemisphere projections of AMS data from Mt Bambouto with inferred flow direction using field indicators and imbrication of magnetic foliation (normal fabrics) are also shown; squares, triangles and circles represent K_1, K_2 and K_3 respectively; filled symbols represent means of K_1, K_2 and K_3. In every stereoplots of AMS axes, values of magnetic foliation (F) and lineation (L) are also indicated

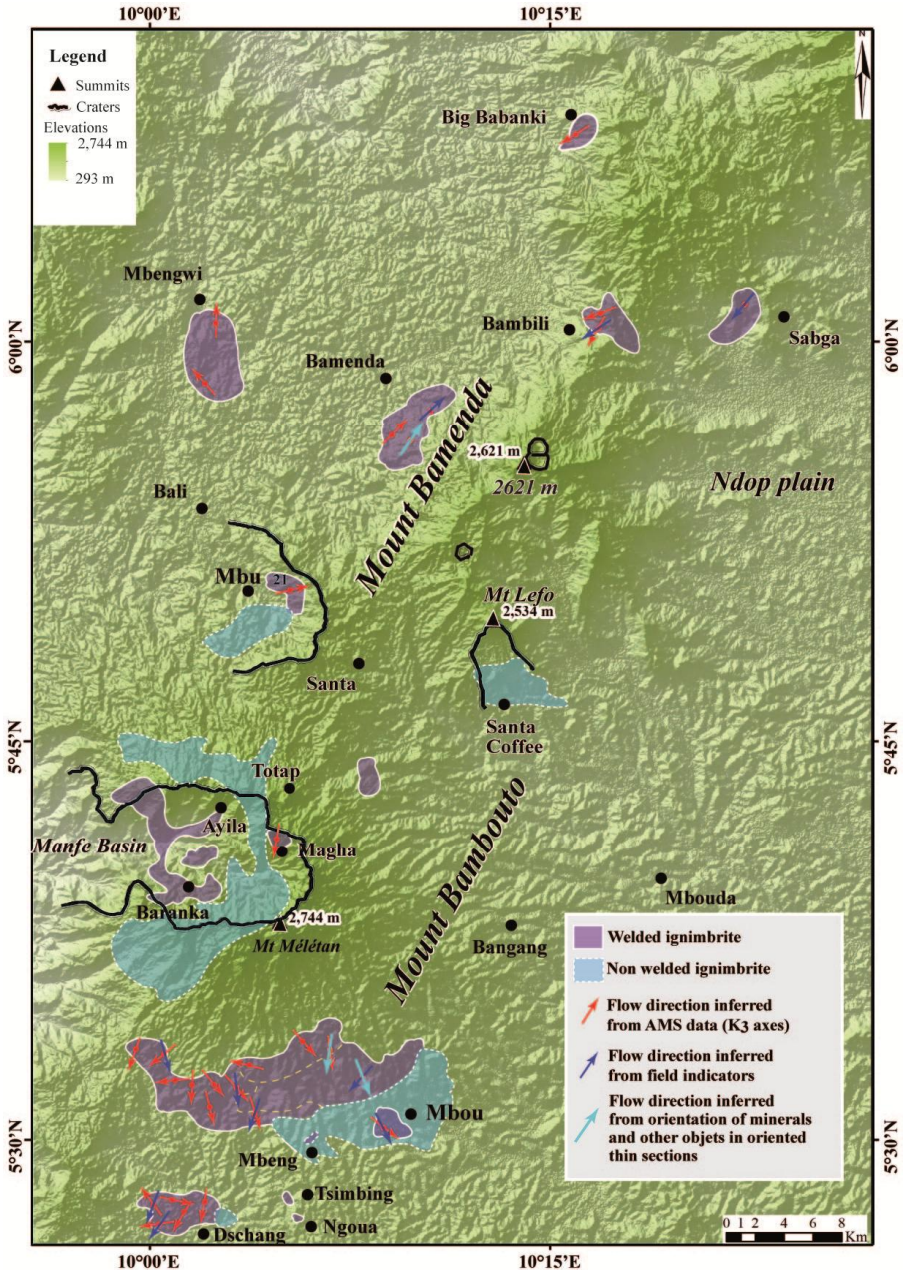

Fig. 8. DEM of study area showing mean flow directions inferred from the orientation of AMS data, field indicators and orientation of minerals and other objects in oriented thin sections

Vulnerability map (Fig. 10) highlights the stake of the study area. The stake includes humans (Children, men and women), houses and their respective equipment and, farms and cattle. Major towns are found in the downslope areas of the volcanoes whereas small towns/villages are found on the upper slopes of the volcanoes. Other stake that can be taken into account is the forest and breeding areas [73].

The risks map (Fig. 11) highlights the risk zones in the study areas. In case of the resumption of a volcanic eruption, certain human and natural patrimonies developed on the ancient pyroclastic flows are more exposed to the damage (high risks zone). Moreover, the inhabitants living on the trajectory of the former flow are also exposed to damage (Low risks zone).

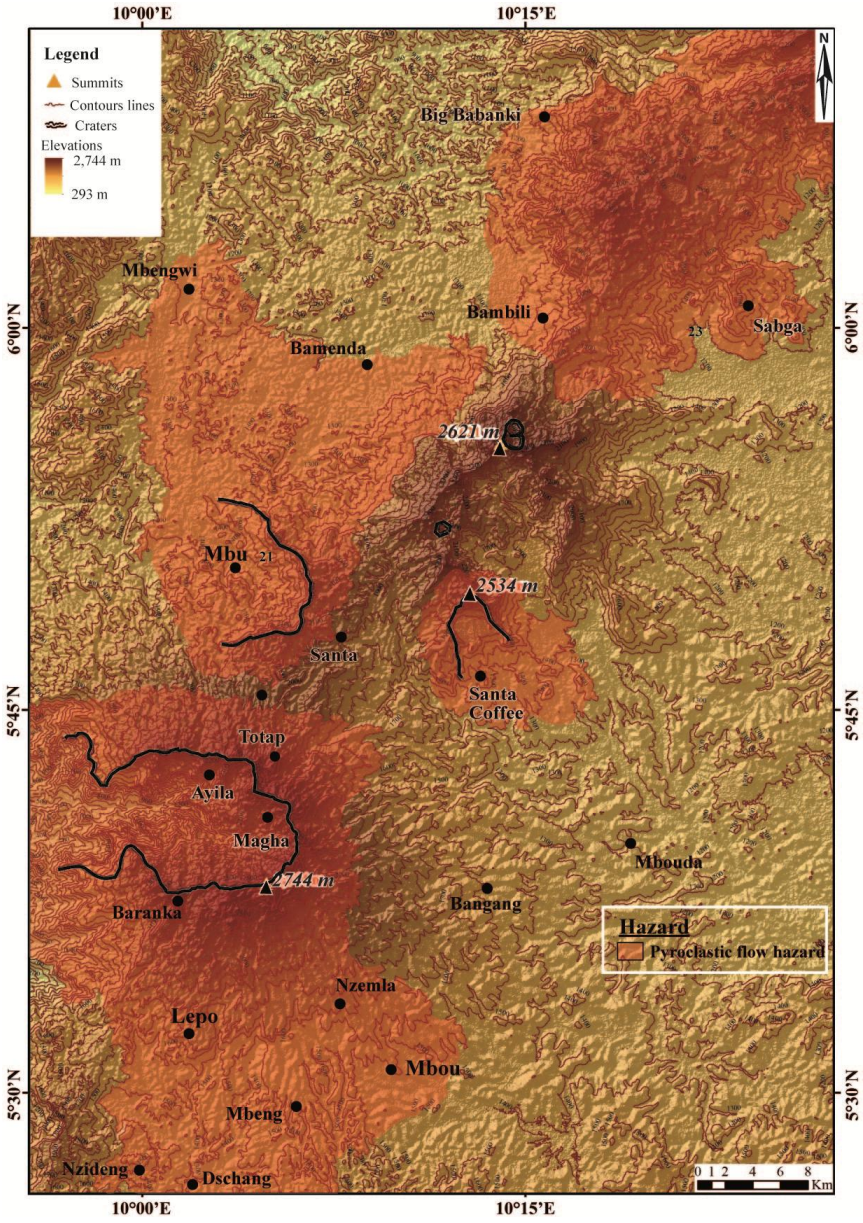

Fig. 9. Hazard map of the study area showing the probably deposits zones of pyroclastic density currents

4.2.2 Assessment

The first risk assessment work in the study area was carried out by Zangmo et al. [74,75] in the calderas of Mt Bambouto and Lefo. The Bambouto and Bamenda volcanoes and its nearby surroundings are densely populated with more than 1250000 inhabitants. The information for the location and inventory of the exposed elements, followed by the examination of the different values (strategic, human, environmental, economic, social and monetary) was achieved by field surveys from the relevant Cameroonian government departments and completed by concerned organizations. Population (places of sporadic concentrations of people and urbanized areas, such as markets, schools, stadiums main centres of worship), networks infrastructures and buildings (roads and bridges, housing, telecommunications relays, water-supply systems, power networks), breeding activities, main centres of economic

and financial interest (factories, banks, tourist centres), strategic buildings for crisis management (army and security, governance, health centres), farmland and natural environment (industrial plantations, food crops, vegetation and hydrography) are the main elements considered by the authorities of Cameroon as being the most important. According to the Ministry of livestock, fisheries and animal industries of Cameroon, in the departments covered by Mts Bto and Bamenda, the cost of livestock is generally estimated at around 8.5 billion FCFA ($U14.0369 million).

Assessing the value of the different element-at-risk was focused on information obtained from the several organizations and services responsible for the social system (Table 2). It is therefore possible to assess by this technique of calculation the total capital budget (updated to 2020) of this different elements within the study area at about 4193 billion FCFA or $US9.93 billion.

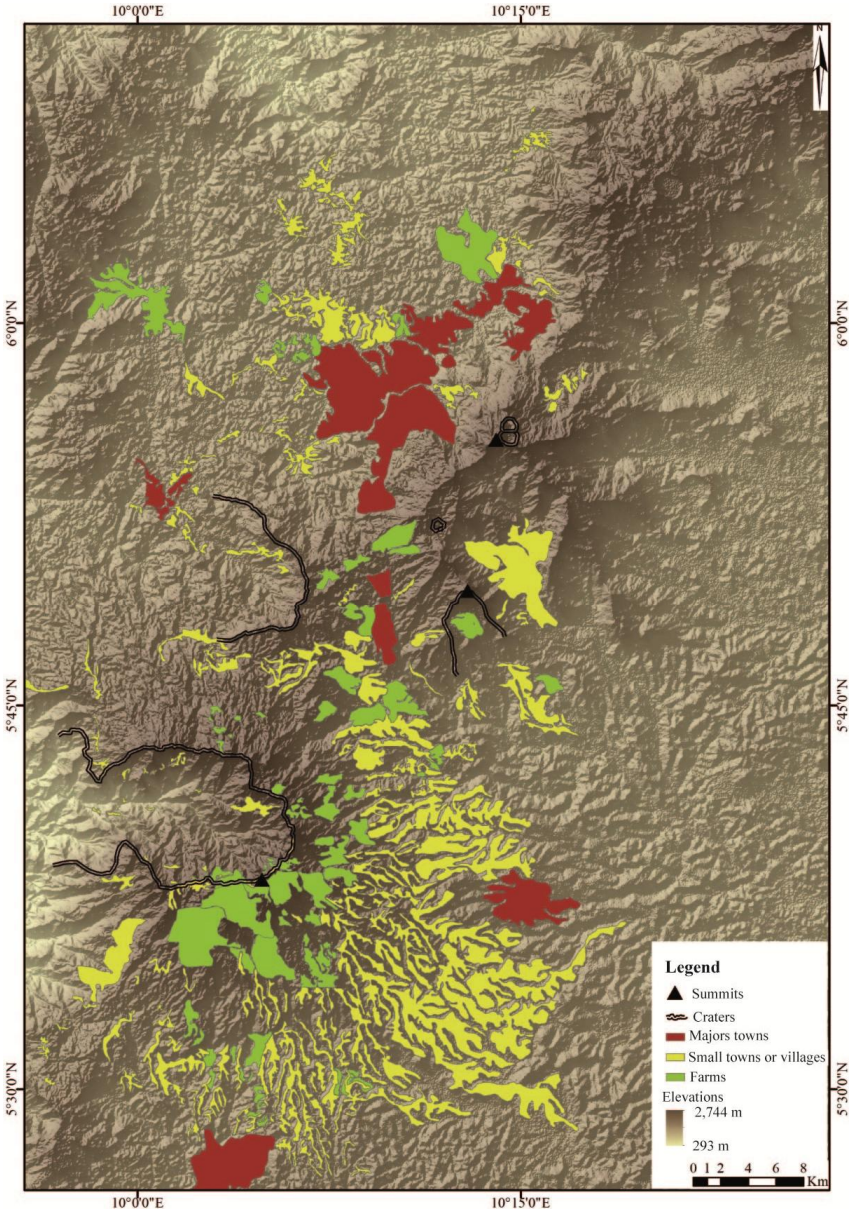

Fig. 10. Vulnerablity map of Bamenda and Bambouto volcanoes

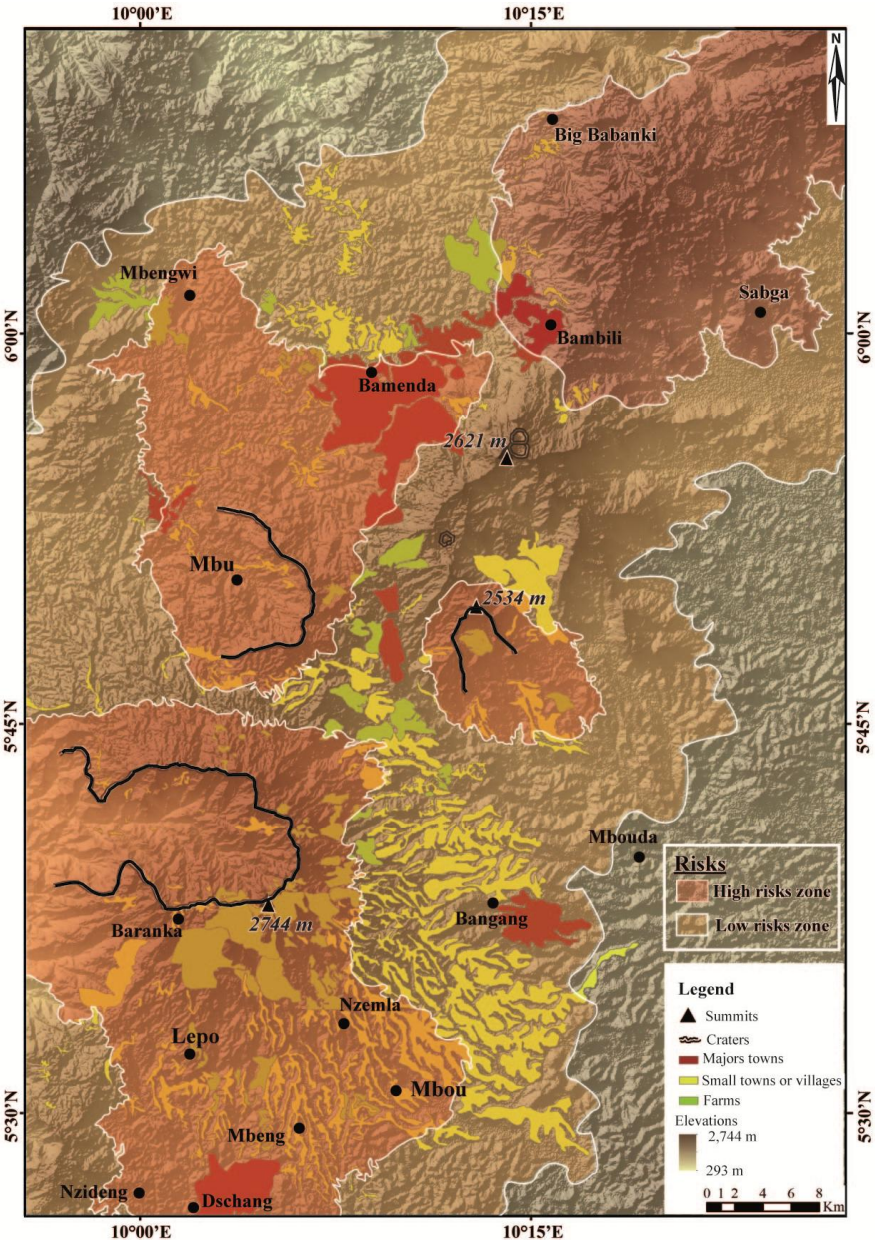

Fig. 11. Risks map of Bambouto and Bamenda volcanoes

Table 2. Average construction costs in the study area (updated in 2020)

Type of construction (houses and roads)	Cost per m^2 of housing and road (FCFA). (1,000 FCFA = $US1.65140)
Wooden or clay-brick cabin without foundations	25,000 - 45,000
Wooden or clay-brick cabin on a masonry foundation	45,000 - 70,000
Mixed construction building (breeze-blocks and wood or sheet metal)	85,000
‘‘Standard’’ house of breeze-blocks and reinforced concrete (R0-R1-R2-R3)	155,000 per storey
Road	Tarred: 2850; Not tarred: 750

Source: [73]

5. CONCLUSION

With the help of ASM study, field indicators and orientation of minerals and other objects in oriented thin sections, the palaeoflow of pyroclastic density currents were highlighted in the deposits of ignimbrites of Miocene age constituted in most cases by remnant blocks of PDCs deposits. The map of mean flow directions of pyroclastic flow obtained from each AMS station was used to realize vulnerability, hazard and risks maps of Bambouto and Bamenda volcanoes. The high density of population in the Mts Bamenda and Bambouto regions (1,250,000 inhabitants) increasing the vulnerability level for the future ignimbritic eruptions. Therefore, the risk will be high if the hazards will happened. The economical assets of this volcanic region gave rise to the settlement of active population that leads the cost-effective breeding and farming activities. This situation increases the level of risk which is evaluated at roughly $US9.93 billion.

COMPETING INTERESTS

Authors have declared that no competing interests exist.

REFERENCES

1. Moundi A, Wandji P, Bardintzeff J-M, Ménard J-J, Okomo Atouba LC, Farouk Mouncherou O, Reusser E, Bellon H, Tchoua FM. Les basaltes Eocène à affinité transitionnelle du plateau Bamoun, témoins d'un réservoir mantellique enrichi sous la ligne volcanique du Cameroun. Comptes Rendus Géoscience. 2007;339: 831–837.
2. Fosso J, Ménard J-J, Bardintzeff J-M, Wandji P, Tchoua FM, Bellon H. Les laves du mont Bangou: Une première manifestation volcanique Eocène, à affinité transitionnelle, de la Ligne du Cameroun. Comptes Rendus Géoscience. 2005;337:315–325.
3. Sato H, Aramaki S, Kusakabe M, Hirabayashi J, Sano Y, Nojiri Y, Tchoua F. Geochemical difference of basalts between polygenetic and monogenetic volcanoes in the central part of the Cameroon volcanic line. Geochemistry Journal. 1990;24:357–370.
4. Marzoli A, Piccirillo EM, Renne PR, Bellieni G, Iacumin M, Nyobe JB, Tongwa AT. The Cameroon volcanic line revisited: Petrogenesis of continental basaltic magmas from lithospheric and asthenospheric mantle sources. Journal of Petrology. 2000;41:87–109.
5. Graser G, Potter J, Köhler J, Markl G. Isotope, major, minor and trace element geochemistry of late-magmatic fluids in the peralkaline Ilimaussaq intrusion, South Greenland. Lithos. 2008;106:207–221.
6. Kamgang P, Njonfang E, Nono A, Gountié Dedzo M, Tchoua FM. Petrogenesis of a silicic magma system: Geochemical evidence from Bamenda Mountains, NW Cameroon, Cameroon Volcanic Line. Journal of African Earth Sciences. 2010;58:285-304.
7. Kamgang P, Chazot G, Njonfang E, Ngongang NBT, Tchoua FM. Mantle sources and magma evolution beneath the Cameroon volcanic line: Geochemistry of mafic rocks from the Bamenda mountains (NW Cameroon). Gondwana Research. 2013;24:727–741.
8. Njome MS, De Wit MJ. The Cameroon line: Analysis of an intraplate magmatic province transecting both oceanic and continental lithospheres: Constraints, controversies and models. Earth-Science Review.
   DOI: 10.1016/j.earscirev.2014.09.003
9. Asaah ANE, Yokoyama T, Aka FT, Usui T, Wirmvem MJ, Chako Tchamabé B, Ohba T, Tanyileke G, Hell JV. A comparative review of petrogenetic processes beneath the Cameroon volcanic line: Geochemical constraints. Geoscience Frontiers. 2015;6:557–570.
10. Merle R, Marzoli A, Aka FT, Chiaradia JM, Reisberg L, Castorina F, Jourdan F, Renne PR, N'ni J, Nyobe JB. Mt Bambouto Volcano, Cameroon line: Mantle source and differentiation of within-plate alkaline rocks. Journal of Petrology. 2017;58:933–962.
11. Gountié Dedzo M, Asaah ANE, Fozing EM, Tchamabé BC, Tefogoum Zangmo G. Petrology and geochemistry of lavas from Gawar, Minawao and Zamay volcanoes of the northern segment of the Cameroon volcanic line (Central Africa): Constraints on mantle source and geochemical evolution. Journal of African Earth Sciences. 2019;153:31-41.
12. Gountié Dedzo M, Nédélec A, Nono A, Njanko T, Font E, Kamgang P, Njonfang E, Launeau P. Magnetic fabrics of the Miocene ignimbrites from West-Cameroon: Implications for pyroclastic flow source and

sedimentation. Journal of Volcanology and Geothermal Research. 2011;203:113-132.

13. Gountié Dedzo M, Nono A, Njonfang E, Kamgang P, Zangmo Tefogoum G, Kagou Dongmo A, Nkouathio DG. Le volcanisme ignimbritique des Monts Bambouto et Bamenda (Ligne du Cameroun, Afrique Centrale): Signification dans la genèse des caldeiras. Bulletin de l'Institut Scientifique, Rabat, Maroc. 2011;33:1-15.
14. Gountié Dedzo M, Njonfang E, Kamgang P, Nono A, Zangmo Tefogoum G, Kagou Dongmo A, Nkouathio DG. Dynamic and evolution of the Mounts Bambouto and Bamenda calderas by study of ignimbritic deposits (West-Cameroon, Cameroon Line). Syllabus Review, Science Series. 2012;3:11-23.
15. Kamgang P. Contribution à l'étude géochimique et pétrologique du massif de Nkogam (pays Bamoun, Ouest-Cameroun). Thèse Doctorat 3^{e} Cycle, Université de Yaoundé; 1986.
16. Dunlop HM. Strontium isotope geochemistry and potassium-argon studies on volcanic rocks from the Cameroon Line, West Africa. PhD Thesis, University of Edinburg, Edinburg; 1983.
17. Lissom J. Etude pétrologique des laves alcalines du massif d'Oku: Un ensemble volcanique de la "Ligne du Cameroun". Thèse Université Pierre et Marie Curie, (Paris VI); 1991.
18. Nono A, Déruelle B, Demaiffe D, Kambou R. Tchabal Nganha volcano in Adamawa (Cameroon): Petrology of a continental alkaline lava series. Journal of Volcanology and Geothermal Research. 1994;60:147-178.
19. Ngako V, Njonfang E, Aka FT, Affaton P, Metuk Nnange J. The North-South paleozoic to quaternary trend of alkaline magmatism from Niger - to Cameroon: Complex interaction between hotspots and Precambrian faults. Journal of African Earth Sciences. 2006;45:241-256.
20. Kamgang P, Njonfang E, Chazot G, Tchoua FM. Géochimie et géochronologie des laves felsiques des monts Bamenda (ligne volcanique du Cameroun). Comptes Rendus Géoscience. 2007;339:659–666.
21. Kagou Dongmo A, Nkouathio D, Pouclet A, Bardintzeff J-M, Wandji P, Tchoua FM, Pouclet A, Bourdier JL. The discovery of late Quaternary basalt on Mount Bambouto: Implications for recent widespread volcanic activity in the Southern Cameroon Line. Journal of African Earth Scence. 2010;57:96–108.
22. Kamgang P, Chazot G, Njonfang E, Tchoua FM. Geochemistry and geochronology of mafic rocks from Bamenda Mountains (Cameroon): Source composition and crustal contamination along the Cameroon Volcanic Line. Comptes Rendus Géoscience. 2008;340:850–857.
23. Gouhier J, Nougier J, Nougier D. Contribution à l'étude volcanologique du Cameroun (« Ligne du Cameroun »-Adamawa). Annales de la Faculté des Sciences de l'Université de Yaoundé, Cameroun. 1974;17:3-48.
24. Tchoua FM. Les explosions phréato-magmatiques dans le volcanisme du Cameroun (Afrique centrale). In: Matheis, G. and Schandelmier, H. (Eds), Current Research in African Earth Science, Balkema, Rotterdam. 1987;271-275.
25. Fitton JG, Dunlop HM. The Cameroon line, West Africa, and its bearing on the origin of oceanic and continental alkali basalt. Earth and Planetary Science Letters. 1985;72:23-38.
26. Marzoli A, Renne PR, Piccirillo EM, Castorina F, Bellieni G, Melfi AJ, Nyobe JB, N'ni J. Silicic magma from the continental Cameroon Volcanic Line (Oku, Bambouto and Ngaoundéré): 40Ar-39Ar dates, petrology, Sr-Nd-O isotopes and their petrogenetic significance. Contributions to Mineralogy and Petrology. 1999;135:133-150.
27. Youmen D, Schmincke H-U, Lissom J, Etame J. Données géochronologiques: Mise en évidence des différentes phases volcaniques au miocène dans les Monts Bambouto (Ligne du Cameroun). Science, Technologie et Développement. 2005;11:49-57.
28. Nkouathio DG, Kagou Dongmo A, Bardintzeff J-M, Wandji P, Bellon H. Evolution of volcanism in graben and horst structures along the Cenozoic Cameroon Line (Africa): Implications for tectonic evolution and mantle source composition. Mineralogy and Petrology. 2008;94:287–303.
29. Branney MJ, Kokelaar P. Pyroclastic density currents and the sedimentation of ignimbrites. Geological Society of London Memoirs. 2002;27.
30. Schminke H.-U. Volcanism. Springer-Verlag, Berlin-Heidelberg; 2004.

31. Wilson CJN, Houghton BF. Pyroclast transport and deposition. In: Sigurdsson H, (Ed.) Encyclopedia of Volcanoes, Academic Press. 2000;545–554.
32. Carey S. Transport and deposition of tephra by pyroclastic flows and surges. Sedimentation in volcanic settings. SEPM Special Publication. 1991;45:39-57.
33. Druitt TH. Pyroclastic density currents. In: Gilbert, J.S., Sparks, R.S.J. (Ed) The physics of explosive volcanic eruptions. Geological Society of London Special Publications. 1998;145:145–182.
34. Belousov A, Voight B, Belousova M, Petukhin A. Pyroclastic surges and flows from the 8–10 May 1997 explosive eruption of Bezymianny volcano, Kamchatka, Russia. Bulletin of Volcanology. 2002;64:455–471.
35. Burgisser A, Bergantz GW. Reconciling pyroclastic flow and surge: The multiphase physics of pyroclastic density currents. Earth Planet. Sci. Lett. 2002;202:405–418.
36. Fisher RV. Transport and deposition of a pyroclastic surge across an area of high relief: The 18 May 1980 eruption of Mount St. Helens, Washington. Geol. Soc. Am. Bull., 1990;92:938–954.
37. Dellino P, La Volpe L. Structures and grain size distribution in surge deposits as a tool for modelling the dynamics of dilute pyroclastic density currents at La Fossa di Vulcano. Journal of Volcanology and Geothermal Research. 2000;96:57–78.
38. Valentine GA, Fisher RV. Pyroclastic surges and blasts. In: Sigurdsson, H. (Ed.) Encyclopedia of Volcanoes, Academic Press. 2000;571–580.
39. Choux C. Sédimentation et ségrégation dans les écoulements de suspension concentrée. Approche expérimentale et applications volcanologiques. Thèse Doctorat Université Blaise Pascal Clermont-Ferrand II; 2001.
40. Walker GPL. Ignimbrite types and ignimbrite problems. Journal of Volcanology and Geothermal Research. 1983;17:65–88.
41. Wilson CNJ. Emplacement of the Taupo ignimbrite. Nature, 1997;385:306–307.
42. Fisher RV, Schmincke HU. Pyroclastic rocks. Springer-Verlag, New York; 1984.
43. Cas RFA, Wright JV. Volcanic successions, modern and ancient; a geological approach to processes, products and successions. Chapman and Hall (Eds), London; 1987.
44. Mellors RA, Waitt RB, Swanson DA. Generation of pyroclastic flows and surges by hot-rock avalanches from the dome of Mount St. Helens volcano, USA. Bulletin of Volcanology. 1988;50:14–25.
45. Calder ES, Cole PD, Dade WB, Druitt TH, Hoblitt RP. Mobility of pyroclastic flows and surges at Soufrière Hills Volcano, Montserrat. Geophysical Research Letters. 1999;26:537–540.
46. Wilson CNJ, Houghton BF, Kamp PJJ, Mcwilliams MO. An exceptionally widespread ignimbrite with implications for pyroclastic flow emplacement. Nature. 1995;378:605-607.
47. Freundt A, Wilson CJN, Carey SN. Ignimbrites and block-and-ash flow deposits. In: Sigurdsson, H. (Eds.), Encyclopedia of Volcanoes. Academic Press, San Diego. 2000;581-599.
48. Jelinek V. Characterization of the magnetic fabric of rocks. Tectonophysics. 1981;79:563–7.
49. Ellwood BB. Estimate of flow direction for calc-alkaline welded tuffs and paleomagnetism data reliability from anisotropy of magnetic susceptibility measurements: Central San Juan Mountains, Southwest Colorado. Earth Planetary Science Letters. 1982;59:303-314.
50. Knight MD, Walker GPL, Ellwood BB, Diehl-Jimmy F. Stratigraphy, paleomagnetism and magnetic fabric of the Toba tuffs; constraints on the sources and eruptive style. Journal of Geophysical Research. 1986;91:10355-10382.
51. McDonald WD, Palmer HC. Flow directions in ash flow tuffs: A comparison of geological and magnetic susceptibility measurements. Tshirege member (upper Bandelir Tuff) Valles caldera. New Mexico. USA. Bulletin of Volcanology. 1990;53:45–59.
52. Seaman SJ, Mcintosh WC, Geissman JW, Williams ML, Elston WE. Magnetic fabrics of the Bloodgood Canyon and Shelley Peak Tuffs, South-Western New Mexico: Implications for emplacement and alteration processes. Bulletin of Volcanology. 1991;53:460-476.
53. Wolff JA, Ellwood BB, Sachs SD. Anisotropy of magnetic susceptibility in welded tuffs: Application to a welded-tuff dyke in the Tertiary Tram-Pecos Texas volcanic province, USA. Bulletin of Volcanology. 1989;51:299-310.

54. Palmer HC, MacDonald WD. Anisotropy of magnetic susceptibility in relation to source vents of ignimbrites: Empirical observations. Tectonophysics. 1999;307: 207-218.
55. Rochette P. Magnetic susceptibility of the rock matrix related to magnetic fabric studies. Journal of Structural Geology. 1987;9:1015–1020.
56. Rochette P, Jackson M, Aubourg C. Rock magnetism and the interpretation of anisotropy of magnetic susceptibility. Rev. Geophys. 1992;30:209-26.
57. Tarling DH, Hrouda F. The magnetic anisotropy of rocks. Capman and Hall, London; 1993.
58. Bouchez JL. Granite is never isotropic: An introduction to AMS studies of granitic rocks. In: Bouchez JL, Hutton DHW, Stephens WE, Eds. Granite: From segregation of melt to emplacement fabrics. Kluwer: Dordrecht. 1997;96-112.
59. Giordano G, Porreca M, Musacchio P, Mattei M. The Holocene Secche di Lazzaro phreatomagmatic succession (Stromboli, Italy): evidence of pyroclastic density current origin deduced by facies analysis and AMS flow directions. Bulletin of Volcanology. 2008;70:1221-36.
60. Hillhouse JW, Wells RE. Magnetic fabric, flow directions, and source area of the lower Miocene Peach Springs Tuff in Arizona, California and Nevada. Journal of Geophysical Research. 1991;96:12443-12460.
61. Ort MH. Eruptive processes of caldera formation in a nested downsag-collapse caldera: Cerro Panizos, Central Andes Mountains. Journal of Volcanology and Geothermal Research. 1993;56:221-252.
62. Le Pennec JL, Chen Y, Diot H, Froger JL, Gourgaud A. Interpretation of anisotropy of magnetic susceptibility fabric of ignimbrites in terms of kinematic and sedimentological mechanisms: An Anatolian case-study. Earth Planetary Science Letters. 1998;157:105-127.
63. Henry B. Contribution à l'étude des propriétés magnétigues de roches magmatiques des Alpes: Conséquences structurales, régionales et générales Trav Lab Tectonphysique. CRE: Paris. 1980;1-528.
64. Thompson R, Oldfield F. Environmental magnetism. Allen and Unwin, London; 1986.
65. Alva-Valdivia LM, Rosas-Elguera J, Bravo-Medina T, Urrutia-Fucugauchi J, Henry B, Caballero C, Rivas-Sanchez ML, Goguitchaichvili A, López-Loera H. Paleomagnetic and magnetic fabric studies of the San Gaspar ignimbrite, Western Mexico: Constraints on emplacement mode and source vents. Journal of Volcanology and Geothermal Research. 2005;147:68-80.
66. Wang X, Roberts J, Schmidt P. Flow directions of carboniferous ignimbrites, Southern New England Oregon, Australia, using anisotropy of magnetic susceptibility. Journal of Volcanology and Geothermal Research. 2001;110:1-25.
67. Rochette P, Aubourg C, Perrin M. Is this magnetic fabric normal? A review and case studies in volcanic formations. Tectonophysics 1999;307:219-234.
68. Robin PY. Determination of fabric and strain ellipsoids from measured sectional ellipses - theory. Journal of Structural Geology. 2002;24:531-544.
69. Launeau P, Robin PY. Determination of fabric and strain ellipsoids from measured sectional ellipses - implementation and applications. Journal of Structural Geology. 2005;27:2223-2233.
70. Buesch DC. Incorporation and redistribution of locally-derived lithic fragments within a pyroclastic flow. Geological Society of America Bulletin. 1992;104:1193-1207.
71. Ort MH, Orsi G, Pappalardo L. Anisotropy of magnetic susceptibility studies of depositional processes in the Campanian Ignimbrite, Italy. Bulletin of Volcanology. 2003;65:55-72.
72. Petronis MS, Geissman JW. Anisotropy of magnetic susceptibility data bearing on the transport direction of mid-tertiary regional ignimbrites, Candelaria Hills area, West-Central Nevada. Bulletin of Volcanology. 2009;71:121.
73. Dedzo MG, Kamgang P, Njonfang E, Tefogoum GZ, Dongmo AK, Nkouathio DG. Mapping and assessment of volcanic hazards related to the ignimbritic eruption by AMS in Bambouto Volcano (Cameroon Volcanic Line). The Open Geology Journal. 2013;7(1).
74. Zangmo Tefogoum G, Kagou Dongmo A, Nkouathio DG, Wandji P. Typology of Natural hazards and assessment of associated risks in the Mounts Bambouto

Caldera (Cameroon Line, West-Cameroon). Acta Geologica Sinica. 2009;5:1008-1016.

75. Zangmo Tefogoum G, Nkouathio DG, Kagou Dongmo A, Gountié Dedzo M, Kamgang P. Study of multi-origin hazards and assessment of associated risks in the Lefo Caldera (Bamenda Volcano, Cameroon Line). International Journal of Geosciences. 2014;5:1300-1314.

Peer-review history:
The peer review history for this paper can be accessed here:
http://www.sdiarticle4.com/review-history/55452